Development 138, 55-64 (2011) doi:10.1242/dev.055533

The repression of Notch signaling occurs via the destabilization of mastermind-like 1 by Mesp2 and is essential for somitogenesis

Nobuo Sasaki[1], Makoto Kiso[1], Motoo Kitagawa[2] and Yumiko Saga[1,3,*]

SUMMARY

The rostro-caudal polarity within a somite is primarily determined by the on/off state of Notch signaling, but the mechanism by which Notch is repressed has remained elusive. Here, we present genetic and biochemical evidence that the suppression of Notch signaling is essential for the establishment of rostro-caudal polarity within a somite and that Mesp2 acts as a novel negative regulator of the Notch signaling pathway. We generated a knock-in mouse in which a dominant-negative form of Rbpj is introduced into the *Mesp2* locus. Intriguingly, this resulted in an almost complete rescue of the segmental defects in the *Mesp2*-null mouse. Furthermore, we demonstrate that Mesp2 potently represses Notch signaling by inducing the destabilization of mastermind-like 1, a core regulator of this pathway. Surprisingly, this function of Mesp2 is found to be independent of its function as a transcription factor. Together, these data demonstrate that Mesp2 is a novel component involved in the suppression of Notch target genes.

KEY WORDS: Mastermind-like 1, Mesp2, Notch signaling, Somitogenesis, Mouse

INTRODUCTION

In the developing vertebrate embryo, the somites are the most obviously segmented structure and give rise to metameric structures such as the vertebrae and ribs. The somites are rhythmically produced from the presomitic mesoderm (PSM) under the control of the so-called 'segmentation clock', which is characterized by the periodic expression of genes involved in the Notch, Wnt and Fgf signaling pathways (reviewed by Dequeant and Pourquie, 2008; Lewis, 2008). In the posterior PSM of the mouse embryo, the transcripts of Notch signaling components such as Hes7, a basic helix-loop-helix (bHLH)-type transcription factor and Lfng (a glycosyltransferase implicated in Notch receptor modification), oscillate and travel in a posterior-to-anterior direction during each segmentation cycle (Bessho et al., 2003). Notch activity also oscillates and travels in the posterior PSM (Morimoto et al., 2005). Once Notch signals reach the anterior PSM, they are arrested at the future segmentation point, where temporal information is translated into the spatial pattern that generates segmented somites (Saga and Takeda, 2001).

Each somite is subdivided into anterior (rostral) and posterior (caudal) compartments and this division is already determined prior to the physiological segregation of the somite (Aoyama and Asamoto, 1988). The repression and activation of Notch signaling are known to be essential for the establishment of the rostral and caudal compartments of a somite, respectively. Hence, many mutant mice that lack the components of the Notch signaling pathway or have activated Notch1 throughout the PSM show defective rostro-caudal (RC) patterning (Bessho et al., 2001; Evrard et al., 1998; Feller et al., 2008; Takahashi et al., 2000; Zhang and Gridley, 1998). In addition, Mesp2, a bHLH-type transcription factor, is known to be required for the establishment of RC patterning within a somite (Morimoto et al., 2005; Saga et al., 1997; Takahashi et al., 2000). *Mesp2* expression is induced in the anterior PSM just before segmental border formation. Its initial expression domain of approximately one somite in length becomes quickly restricted to the rostral compartment within a presumptive somite. In the absence of *Mesp2*, the rostral identity within a somite is lost and the somite is completely caudalized, indicating that Mesp2 is required to establish the rostral compartment (Saga et al., 1997; Takahashi et al., 2000).

Previous functional studies have shown that Mesp2 plays valuable roles during somitogenesis via its regulation of several target genes as a transcription factor, including the upregulation of *Lfng*, *Epha4* and *Ripply1/2* (Morimoto et al., 2007; Morimoto et al., 2005; Nakajima et al., 2006; Takahashi et al., 2010). Mesp2 has also been shown to have suppressive effects on Notch activity, in part by activating *Lfng* expression in the rostral somite compartment (Morimoto et al., 2005). *Lfng* has been further implicated as a suppressor of the Notch signaling pathway by preventing the formation of cleaved Notch1 (active Notch1, Notch1 intracellular domain, referred to as NICD). *Lfng* expression cycles in the posterior PSM are under the control of Notch signaling, whereas its expression in the anterior PSM is under the control of Mesp2 (Evrard et al., 1998; Hicks et al., 2000; Zhang and Gridley, 1998). To elucidate the functional significance of Lfng acting downstream of Mesp2, we previously generated a knock-in mouse that reproduces the expression pattern of *Lfng* cDNA at the *Mesp2* locus ($Mesp2^{Lfng/+}$) and analyzed $Mesp2^{Lfng/Lfng}$ embryos. However, the activation of Lfng instead of Mesp2 fails to rescue the phenotype of *Mesp2*-null mice and the somites are still caudalized, indicating that Lfng is not responsible for Mesp2 function as a suppressor of Notch signaling (Oginuma et al., 2010). Therefore,

[1]Division of Mammalian Development, National Institute of Genetics, Yata 1111, Mishima, Shizuoka 411-8540, Japan. [2]Department of Molecular and Tumor Pathology, Chiba University Graduate School of Medicine, Chiba 260-8670, Japan. [3]Department of Genetics, SOKENDAI, Yata 1111 , Mishima, Shizuoka 411-8540, Japan.

*Author for correspondence (ysaga@lab.nig.ac.jp)

Accepted 19 October 2010

although there appears to be a requirement for Mesp2 in the suppression of Notch signaling, the action point in this mechanism has remained largely unknown.

MATERIALS AND METHODS

Generation of knock-in and transgenic mice

The knock-in strategy we used to target the *Mesp2* locus is largely similar to our previously described approaches (Takahashi et al., 2000) except that an *Rbpj R218H* or *VP16 Rbpj* cassette was inserted, and these mice do not express *Mesp2* (see Fig. S1 in the supplementary material). The targeting vectors were introduced into embryonic stem (ES) cells (TT2) and the chimeric mice were then crossed with MCH female mice to establish each mouse line. The *Δneo* mouse lines were established by crossing with the CAG-Cre mouse line. Mouse tail or embryo yolk sac genomic DNA was used for genotyping by PCR using the allele-specific primers NeoAR2/Rbpj-3′ for *ΔneoMesp2-R218H* mice and HLH-R3/NeoAL2 for *ΔneoMesp2-VP16* mice. GFP-L1 and GFP-R1 primers were used for TP1 (which includes 12 Rbpj binding sites and a minimum promoter) Venus transgenic mice. These primers are listed in Table S1 in the supplementary material. The primer sets used for genotyping the normal *Mesp2* allele and the *ΔneoMesp2-MCM* mice that contain the *MerCreMer* (a Cre recombinase gene fused to two mutant estrogen-receptor ligand-binding domains) in the *Mesp2* locus have been described previously (Takahashi et al., 2000; Takahashi et al., 2007). Transgenic mice were generated by pronuclear microinjection of the TP1-Venus construct (Kato et al., 1997) into fertilized eggs.

Skeletal preparations and gene expression

Skeletal preparations via Alcian Blue or Alizarin Red staining have been described previously (Saga et al., 1997; Takahashi et al., 2000). Whole-mount in situ hybridization was performed using an InsituPro robot (Intavis), also as described previously (Takahashi et al., 2000). The probes for *Dll1* and *Uncx4.1* were kindly provided by A. Gossler (MH-Hannover, Germany) and P. Gruss (Max-Planck Institute, Germany), respectively.

Analysis of mutant embryos

Embryos were collected, fixed with 4% paraformaldehyde and processed for whole-mount in situ hybridization, cryosectioning or paraffin sectioning (Saga et al., 1997; Takahashi et al., 2000). Immunohistochemistry was performed on frozen sections after antigen retrieval as previously described (Oginuma et al., 2008). Immunostaining using the TSA system (PerkinElmer) was performed with 7 μm frozen sections of embryonic day (E) 10.5 embryos as previously described, with minor modifications (Oginuma et al., 2008). Antibodies against Mesp2 (1:800) (Morimoto et al., 2005), the cleaved NICD (1:400, Cell Signaling Technology) and mastermind-like 1 (Maml1; 1:800; Millipore) were used for immunohistochemistry. The specificity of the anti-Maml1 antibody was confirmed using a *Maml1*-null embryo (Oyama et al., 2007). For the whole-mount detection of TP1-Venus, fixed embryos were incubated with rabbit anti-GFP antibody (1:500; MBL), followed by an Alexa-488-conjugated goat anti-rabbit IgG secondary antibody. Whole-mount immunohistochemistry was performed using rabbit anti-Tbx6 antibodies (1:800; kindly provided by D. L. Chapman, University of Pittsburgh, PA, USA) as described previously, and detected using the Vectastain ABC Kit (Vectastain) and 3,3′-diaminobenzidine (DAB) substrate (White and Chapman, 2005). Whole-mount embryos and sections thereof were observed using a confocal microscope (Carl Zeiss 510) or stereomicroscope (Leica MZ16F).

Western blotting analysis in cultured cells

The expression vectors, modified-HA human MAML1 (Kitagawa et al., 2001), 3×Flag-Mesp2 or the deletion forms of Mesp2, and 3×HA-Mesp1 were constructed using pcDNA3.1 (Invitrogen). NIH3T3 cells were then transfected with these plasmids using Lipofectamine 2000 (Invitrogen). After 24 hours, cellular proteins were extracted as previously described (Kitagawa et al., 2001) and, after separation by SDS-PAGE, were transferred onto Immobilon-P Membranes (Millipore). The membranes were incubated with the primary antibodies anti-Flag (1:8000; Sigma-F3165), anti-HA (1:1000; 12CA5), anti-Myc (1:1000; 9E10; sc-40; Santa Cruz) and anti-tubulin (1:2000, D66; T0198; Sigma). Positive signals were visualized by incubation with an appropriate secondary antibody conjugated with horseradish peroxidase followed by detection using an ECL Western Blotting Analysis System (GE Healthcare). In some cases, the membranes were stripped and reblotted.

Immunocytochemistry

NIH3T3 cells seeded in Lab-Tek Chamber Slides (Nalge Nunc) were transfected with plasmids using Lipofectamine 2000 according to the manufacturer's instructions (Invitrogen). For immunostaining, cells were fixed with 4% paraformaldehyde for 30 minutes on ice followed by staining with anti-HA (1:100; 12CA5) and anti-Flag (1:100; Sigma-F7425) primary antibodies overnight at 4°C and then Cy3-conjugated sheep anti-mouse IgG and an Alexa-488-conjugated goat anti-rabbit IgG secondary antibody. The stained cells were analyzed with a laser-scanning microscope (Zeiss 510).

Tamoxifen treatment and western blotting analyses of Mesp2 misexpressing embryos

Tamoxifen (Sigma) was dissolved in pre-warmed sesame oil (Sigma) to make a 10 mg/ml solution and stored at 4°C. To induce Cre activity in bi-transgenic Cre-ERT2 and CAG-CAT-Mesp2 (Nakajima et al., 2006) mice, pregnant females were injected with tamoxifen: 3 mg of tamoxifen per pregnant female was administered at E8.5 or E9.5 and the animals were sacrificed at E10.5. For western blotting analysis, whole embryos were homogenized using a tissue grinder in whole-cell extraction buffer containing protease inhibitors (Kitagawa et al., 2001). After 90 minutes of gentle agitation at 4°C, the supernatants were collected by centrifugation and its protein concentrations were measured using a standard protein assay kit (Bio-Rad). Each cell extract preparation (50 μg) was then loaded onto a 7% SDS-PAGE gel and electroblotted onto an Immobilon-P Membrane (Millipore). Western blotting was performed using the primary antibodies anti-Maml1 (1:500; Bethyl-A300-673A) and anti-tubulin (1:2000; D66; Sigma-T0198).

Semi-quantitative RT-PCR

RNAs were prepared using an RNeasy Mini Kit (Qiagen). cDNA was then generated using Superscript III Reverse Transcriptase (Invitrogen). Subsequent PCR was performed using the primers HA-Maml1 Fw01 and HA-Maml1 Rv01 for the *HA-Maml1* gene, and G3PDH Fw and G3PDH Rv for the *G3PDH* control. The primer sequences are described in Table S1 in the supplementary material.

RESULTS

Rescue of *Mesp2*-null defects in dominant-negative *Rbpj* knock-in mice

To determine whether the suppression of Notch signaling underlies the mechanism by which Mesp2 confers the rostral identity to a somite in vivo, we established two mouse lines that express the dominant-negative form (*Rbpj R218H*; abbreviated as *R218H*) and constitutively active form (*VP16 Rbpj*; abbreviated as *VP16*) of the *Rbpj* gene (also referred to as *CBF1* or *CSL*) in the place of *Mesp2* (see Fig. S1 in the supplementary material). The rationale for this approach was that Rbpj is a potent downstream effector of Notch signaling (Chung et al., 1994; Kato et al., 1997). It has also been reported that the R218H mutant lacks DNA binding ability but still competes with endogenous Rbpj for binding to the NICD or an unknown cofactor (Kato et al., 1997).

We first evaluated the expression pattern of several marker genes to confirm that our knock-out and knock-in strategies had been successful (Fig. 1A-P). *Mesp2* expression was lost as expected (Fig. 1A-D), whereas *Mesp1* (a homolog of *Mesp2*) expression was upregulated in these knock-in mice (Fig. 1E-H), probably owing to the upregulation of Tbx6 in the absence of Mesp2 (Fig. 1I-L) (Oginuma et al., 2008; Saga, 1998; Takahashi et al., 2010). The

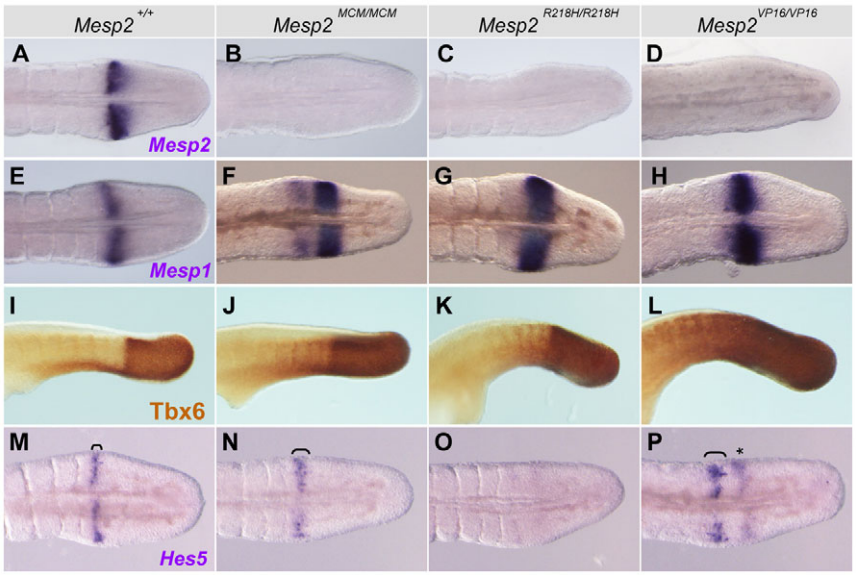

Fig. 1. Appropriate levels of gene expression are achieved following the integration of dominant-negative and constitutively active forms of Rbpj at the *Mesp2* locus. (**A-P**) Whole-mount in situ hybridization and immunohistochemical analyses were conducted using E11.5 mouse embryos of the indicated genotypes: *Mesp2*$^{+/+}$ (A,E,I,M) *Mesp2*$^{MCM/MCM}$ (B,F,J,N), *Mesp2*$^{R218H/R218H}$ (C,G,K,O) and *Mesp2*$^{VP16/VP16}$ (D,H,L,P). Analyses were conducted for *Mesp2* (A, *n*=17; B, *n*=8; C, *n*=4; D, *n*=4), *Mesp*1 (E, *n*=6; F, *n*=4; G, *n*=4; H, *n*=4), Tbx6 protein (I, *n*=3; J, *n*=3; K, *n*=2; L, *n*=2) and *Hes5* (M, *n*=5; N, *n*=2; O, *n*=4; P, *n*=4). Brackets show the width of the *Hes5*-expressing region (M,N,P). An additional *Hes5* band (asterisk) was always observed in *Mesp2*$^{VP16/VP16}$ mice (P).

expression of *Hes5*, a target of Notch signaling, normally observed as a single band in the anterior PSM in wild type (Fig. 1M), was slightly expanded in *Mesp2*$^{MCM/MCM}$ mice (Fig. 1N) (Takahashi et al., 2007), downregulated in *Mesp2*$^{R218H/R218H}$ mice (Fig. 1O) and upregulated as two striped bands in *Mesp2*$^{VP16/VP16}$ mice (Fig. 1P). These gene expression data confirmed that *Mesp2* expression was lost from *Mesp2*$^{R218H/R218H}$ and *Mesp2*$^{VP16/VP16}$ mice and suggested that Notch signaling activity might be repressed and activated by R218H and VP16, respectively.

Next, we examined the resulting skeletal phenotypes of these knock-in mice as the RC pattering of vertebra is known to correlate with Notch signaling activity in the Mesp2-expressing domain. In the absence of *Mesp2* (*Mesp2*$^{MCM/MCM}$), the pedicles of the neural arches and the proximal region of the ribs fused with their neighbors owing to the upregulation of Notch activity, and the mice died shortly after birth as previously reported (Fig. 2B,F,J) (Saga et al., 1997; Takahashi et al., 2007). Intriguingly however, we found that the *Mesp2*$^{R218H/R218H}$ knock-in mice showed a marked rescue of this vertebral phenotype (Fig. 2C,G,K). Although we found some variation in the degree of rescue among these animals, some showed an almost identical morphology to the wild-type controls, and the mice were viable and fertile (compare Fig. 2C,G,K with 2A,E,I). By contrast, the vertebral morphology in the *Mesp2*$^{VP16/VP16}$ knock-in mice showed defects that were far more severe than those of the *Mesp2*$^{MCM/MCM}$ mice and the vertebrae were completely caudalized (Fig. 2D,H,L). These results also indicate that Notch activity is actually repressed by R218H and activated by VP16. However, the heterozygous knock-in mice, *Mesp2*$^{VP16/+}$, showed no abnormalities (Fig. 3A-C). We expected that a half dose of Mesp2 would be sufficient to antagonize VP16. This idea was supported by further comparative analyses among *Mesp2*$^{VP16/+}$, *Mesp2*$^{MCM/MCM}$, *Mesp2*$^{VP16/MCM}$ and *Mesp2*$^{VP16/VP16}$ littermates. The degree of pedicle fusion in *Mesp2*$^{VP16/MCM}$ mice that contains a single copy of VP16 in a *Mesp2*-null background was found to be slightly more severe compared with that of *Mesp2*$^{MCM/MCM}$ mice, but milder than that in *Mesp2*$^{VP16/VP16}$ mice (Fig. 3D-F). These results indicate that VP16 can activate the Notch target gene but that this activity is repressed by a single copy of Mesp2, in addition to the endogenous Rbpj (repressor-type) in *Mesp2*$^{VP16/+}$ mice and by Rbpj alone in *Mesp2*$^{VP16/MCM}$ (see model in Fig. S2 in the supplementary material).

It should be noted that normal segmental borders were generated in *Mesp2*$^{R218H/R218H}$ embryos (Fig. 2O), which were similar to those in wild-type embryos (Fig. 2M). It was necessary to then determine whether this rescue event is also caused by the suppression of Notch activity. We speculate that this apparent rescue event might be due to the upregulation of *Mesp1* (Fig. 1G) as we reported previously that the *Mesp2*-null embryo, which lacks the function of both Mesp1 and Mesp2, fails to form epithelial somites (Takahashi et al., 2005), whereas *Mesp2*$^{MCM/MCM}$ embryos show a milder epithelialization defect (Fig. 2N, arrowheads) owing to the upregulation of *Mesp1* (Takahashi et al., 2007). However, it is noteworthy that, in our current experiments, the somite and skeletal phenotypes of *Mesp2*$^{VP16/VP16}$ mice were not rescued (Fig. 2L,P), even though *Mesp1* is also upregulated in this genetic background (Fig. 1H). We therefore conclude that the rescue event observed in *Mesp2*$^{R218H/R218H}$ mice cannot be only ascribed to the upregulation of *Mesp1*, but is in fact due to the suppression of the canonical Notch signaling pathway.

Rostro-caudal polarity is normally established in *Mesp2*$^{R218H/R218H}$ knock-in mice

To further understand the molecular mechanisms underlying this rescue event, we examined the expression of several genes implicated in the downstream activities of Mesp2 or Notch signaling in the anterior PSM. The expression of *Tbx18* (Fig. 2Q) was found to be almost completely absent in both the *Mesp2*$^{MCM/MCM}$ (Fig. 2R) and *Mesp2*$^{VP16/VP16}$ (Fig. 2T) embryos. However, it was noted that a normal expression pattern of *Tbx18* was observed in *Mesp2*$^{R218H/R218H}$ (Fig. 2S), although at weaker levels than in wild type (Fig. 2Q). The result is consistent with the idea that Tbx18 is required for the maintenance of the rostral properties of the somite (Bussen et al., 2004; Kraus et al., 2001). We also examined the expression of *Dll1* and *Uncx4.1*, caudal markers known to be regulated by Notch signaling (Barrantes et al., 1999; Bettenhausen et al., 1995). In the wild-type embryo, the expression of *Dll1* is persistently strong in the posterior PSM but is downregulated just before the segmental border and is localized in the caudal part of somite number 0 (S0, the prospective somite in the most anterior PSM) and in the segmented somites (Fig. 2U). However, *Dll1* expression is expanded in the rostral compartment of a somite in *Mesp2*$^{MCM/MCM}$ embryos (Fig. 2V). By contrast,

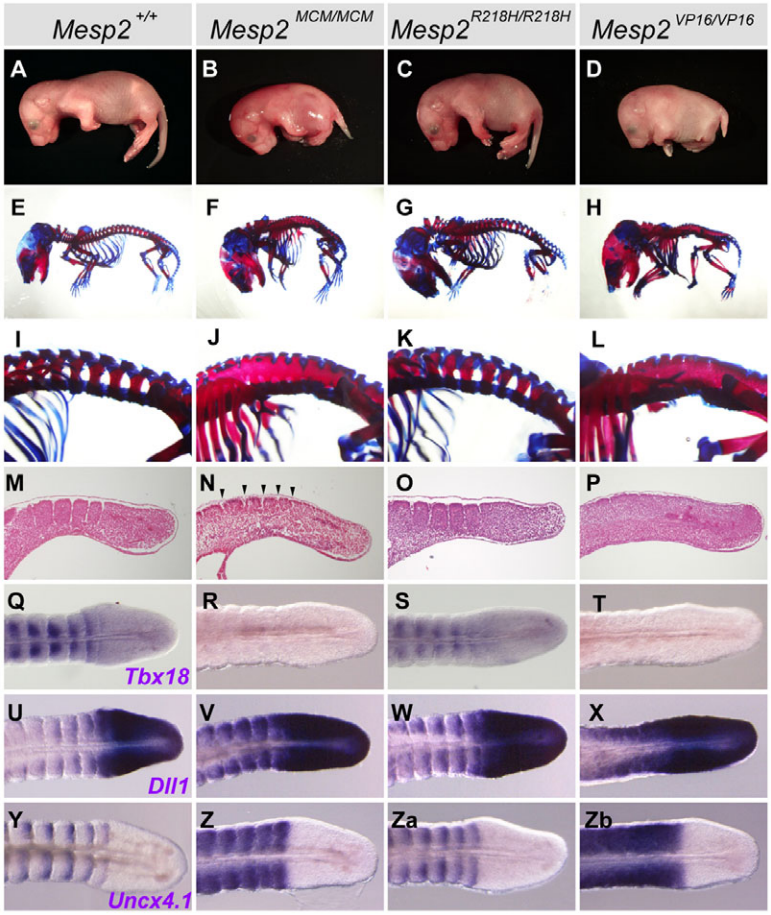

Fig. 2. The *Mesp2*-null defects are almost completely rescued in *Mesp2*^{R218H} homozygous mice.
(**A-L**) Comparisons of the external morphology (A-D), skeletal morphology of the entire body (E-H) and the lumber vertebra (I-L) among E17.5 fetuses of each genotype indicated on the top of the panels (A,E,I, *n*=32; B,F,J, *n*=23; C,G,K, *n*=19; D,H,L, *n*=7). (**M-P**) Hematoxylin- and Eosin-stained sections of the tail region from E10.5 embryos of the indicated genotypes (M, *n*=8; N, *n*=5; O, *n*=9; P, *n*=3). The *Mesp2*$^{MCM/MCM}$ embryo displays a short trunk with a rudimentary tail (B), fused vertebrae (F,J) and partially segmented somites (N, arrowheads). *Mesp2*$^{R218H/R218H}$ embryos show similar morphologies to those of wild type (C,G,K,O). (**Q-Zb**) Whole-mount in situ hybridization analysis using *Tbx18* (Q, *n*=12; R, *n*=7; S, *n*=8; T, *n*=6), a marker for the rostral half of the somites, *Dll1* (U, *n*=14; V, *n*=4; W, *n*=6; X, *n*=4), a marker of the PSM and the caudal half of the somites, and *Uncx4.1* (Y, *n*=22; Z, *n*=8; Za, *n*=8; Zb, *n*=4), a marker of the caudal half of the somites at E11.5. The genotypes are indicated above the panels.

Mesp2$^{R218H/R218H}$ embryos showed a completely normal expression pattern of *Dll1* (Fig. 2W), indicating that Notch signaling is well suppressed in the rostral compartment of a somite in *Mesp2*$^{R218H/R218H}$ embryos. We concluded from these data that the dominant-negative form of Rbpj efficiently competes with endogenous Rbpj, as a result of which Notch signaling is suppressed in the R218H-expressing cells. We also confirmed that the constitutively active form of Rbpj in the *Mesp2*$^{VP16/VP16}$ embryo had the reverse effect upon *Dll1*, the expression of which was expanded anteriorly in the anterior PSM (Fig. 2X). This is similar to the pattern in the *Mesp2*-null embryo (Fig. 2V), indicating an upregulation of Notch activity in the absence of *Mesp2*.

Similar results were revealed by the expression profile of *Uncx4.1*, a known downstream target gene of both Dll1 (activation) and Mesp2 (suppression) (Takahashi et al., 2003). The *Uncx4.1* expression pattern in the *Mesp2*$^{R218H/R218H}$ embryos was segmental, as seen in wild-type embryos, whereas *Mesp2*$^{VP16/VP16}$ and *Mesp2*$^{MCM/MCM}$ embryos showed a disorganized fused pattern (Fig. 2Y-Zb). Therefore, the suppression of Notch signaling by R218H is sufficient to rescue the loss of Mesp2 function and thus to establish RC patterning within a somite, indicating that Mesp2 has a repressive effect upon Notch signal activation (see models in Fig. S2 in the supplementary material).

Mesp2 represses the activation of Notch signaling both in vivo and ex vivo

To dissect the molecular mechanisms underlying the suppression of Notch signaling activation by Mesp2, we established a reporter assay system using NIH3T3 cultured cells, in which Rbpj-mediated transcription can be monitored by TP1 luciferase activity (Kato et al., 1997; Kohyama et al., 2005). The forced expression of a constitutively active form of Notch1 (N1ΔECD) resulted in the upregulation of luciferase activity by up to 80 fold (Fig. 4A). This reporter activity was specifically blocked by both Mesp2 and Mesp1 in a dose-dependent manner but not by the other bHLH-type transcription factor paraxis (Fig. 4A). Subsequently, we examined whether Mesp2 could repress Notch signaling activity in vivo. To monitor Notch activation in the mouse PSM, we generated a TP1-Venus transgenic mouse line and confirmed that the Venus signal could be observed in the caudal half within a somite as expected, although we could not detect oscillating Notch activity using this reporter (Fig. 4B,F). In the *Mesp2*$^{R218H/R218H}$ embryo, R218H was expected to localize in the rostral half of a somite where *Mesp2* is normally expressed. Indeed, the TP1-Venus signal was absent in the rostral half within a somite (Fig. 4D,H). By contrast, the rostral expansion of Venus signals was significant in both the *Mesp2*$^{VP16/VP16}$ (Fig. 4E,I) and *Mesp2*$^{MCM/MCM}$ (Fig. 4C,G) embryos. These results indicate that TP1-Venus appropriately reports the Notch signaling activity involved in the RC pattering of a somite. These data thus provide direct evidence, both ex vivo and in vivo, that Mesp2 acts as a negative regulator of the activation mediated by canonical Notch signaling.

Mesp2 represses Maml1 expression independently of its transactivation activity

We next examined the precise mechanism by which Mesp2 represses Notch signaling activity. We first speculated that Mesp2 might target Rbpj to inhibit Notch signaling as an R218H mutant

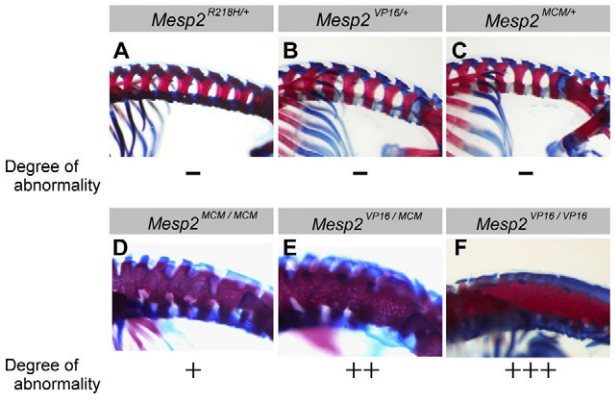

Fig. 3. A single copy of *Mesp2* is sufficient for normal vertebral formation. (**A-F**) Skeletal morphologies of *Mesp2*$^{R218H/+}$ (A, *n*=12), *Mesp2*$^{VP16/+}$ (B, *n*=8), Mesp2$^{MCM/+}$ (C, *n*=8), *Mesp2*$^{MCM/MCM}$ (*Mesp2* knock-out; D, *n*=23), *Mesp2*$^{VP16/MCM}$ (E, *n*=2) and *Mesp2*$^{VP16/VP16}$ (F, *n*=7) mice are shown. Fetuses were prepared at E17.5 and stained with Alizarin Red and Alcian Blue. The degree of abnormalities for each fetus are scored as: – (control), +, ++ or +++. Vertebrae in the heterozygous embryos show a completely normal pattern (A-C, –). *Mesp2* knock-out embryos show fused but partially segmented vertebrae (D, +), and the addition of one copy of *VP16* in the *Mesp2*-null background induced slight alterations in *Mesp2*$^{VP16/MCM}$ (E, ++). By contrast, two copies of *VP16* without *Mesp2* (*Mesp2*$^{VP16/VP16}$) caused severe vertebral fusions (F, +++).

effectively rescued Mesp2 function. We initially examined the possibility of physical interaction between Mesp2 and Rbpj ex vivo, but found no evidence of this association or of interactions with other components involved in the Notch signaling pathway (data not shown). We did notice, however, that the protein expression of mastermind-like 1 (Maml1) was almost completely diminished when co-transfected with either Mesp2 or Mesp1 in NIH3T3 cells (Fig. 5A). Moreover, this effect appeared to be specific to Maml1 and was not observed for NICD, Rbpj or paraxis (see Fig. S3A,B in the supplementary material).

We first examined whether this apparent lack of Maml1 protein is caused by the reduced stability of *Maml1* transcripts. However, RT-PCR analysis ex vivo showed that the expression level of *Maml1* was not affected by Mesp1 nor Mesp2 (Fig. 5B). We further examined the pattern of *Maml1* expression in vivo. In situ hybridization analysis using wild-type embryos revealed that the expression of *Maml1* was ubiquitously observed and not repressed in the anterior PSM where Mesp2 is known to be expressed (Fig. 5C,D). These results indicate that Maml1 protein repression by Mesp1 and Mesp2 does not occur at the transcriptional level or via the instability of mRNA. The other possible mechanism was post-translational destabilization, as it is known that many proteins including Hes7, Mesp2 and Tbx6 are quickly destabilized via proteasome-mediated pathways during somitogenesis (Bessho et al., 2003; Morimoto et al., 2006; Oginuma et al., 2008). To test this possibility, we examined the stability of Maml1 with Mesp2 in the presence of MG132, a potent inhibitor of proteasome pathway. However, we did not observe significant stabilization of Maml1 and its protein levels were rather slightly decreased, which could be partly due to the toxicity of MG132 in NIH3T3 cells (see Fig. S4A in the supplementary material). We tested other protease inhibitors but did not find any that promoted protein stabilization (see Fig. S4B in the supplementary material), indicating that Maml1 is destabilized by Mesp2 via pathways other than the proteasome pathway.

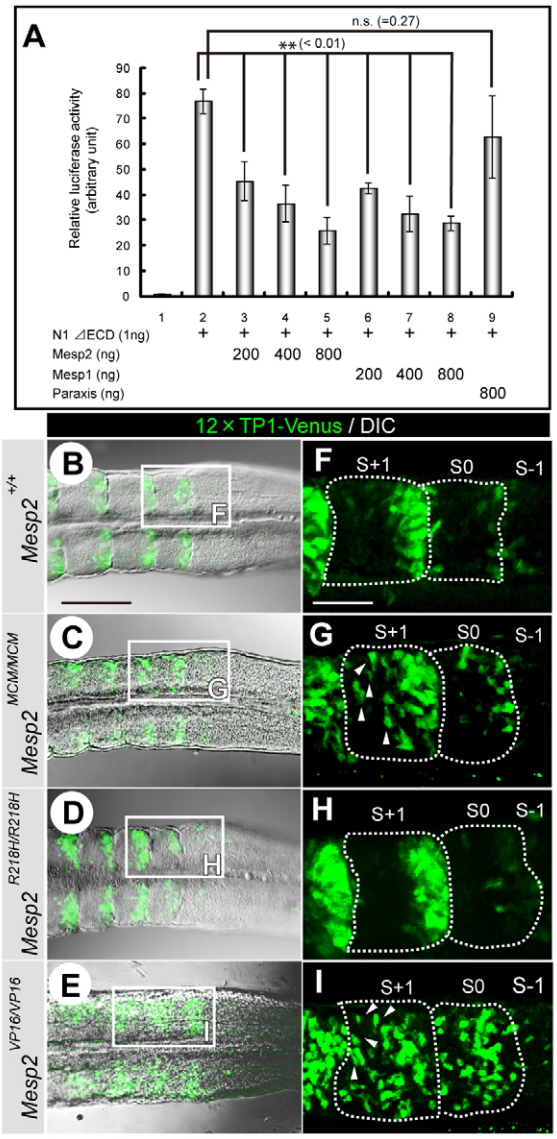

Fig. 4. Mesp2 and Mesp1 have repressive functions during Notch signal activation. (**A**) Luciferase reporter assay using TP1-luciferase. NIH3T3 cells were transfected with the reporter plasmid alone or in combination with the indicated expression vectors. The relative luciferase activities are shown (mean ± s.d. for three independent experiments). (**B-I**) In vivo imaging of Notch activity using TP1-Venus reporter expression (green). The images shown are of differential interference contrast (DIC) and fluorescent overlays from E10.5 embryos of wild-type (B, *n*=4), *Mesp2*$^{MCM/MCM}$*; TP1-Venus* (C, *n*=4), *Mesp2*$^{R218H/R218H}$*; TP1-Venus* (D, *n*=4) and *Mesp2*$^{VP16/VP16}$*; TP1-Venus* (E, *n*=4). F-I are magnified images of the boxed regions in B-E, respectively. Arrowheads indicate ectopic TP1-Venus signals in the rostral region within a somite (G,I). Scale bars: 200 μm in B; 100 μm in F.

Because Mesp2 has already been identified as a transcriptional activator, we predicted that the factor(s) involved in Maml1 destabilization would be induced by Mesp2 (Morimoto et al., 2005; Nakajima et al., 2006). To evaluate this possibility, we generated a mutant Mesp2 (Mesp2ΔbHLH) that lacks both DNA binding and dimerization abilities. If Mesp2 functions as a transcription factor, we expected that Maml1 destabilization would not be observed by the addition of Mesp2ΔbHLH. Unexpectedly however, Maml1

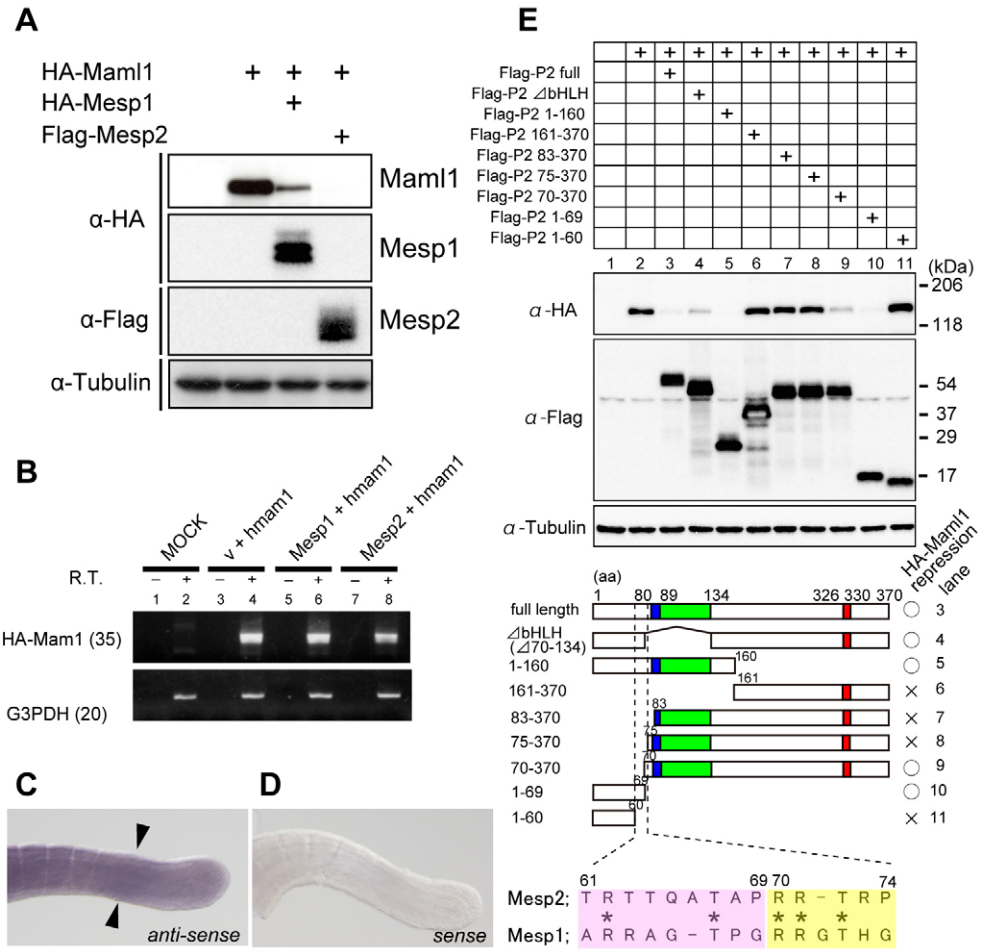

Fig. 5. Mesp2 suppresses Notch signaling activity by inducing the destabilization of Maml1 independently of its DNA binding ability. (**A**) Immunoblotting analysis of exogenous HA-Maml1 expression in the presence of HA-Mesp1 and Flag-Mesp2 in NIH3T3 cells. Tubulin was used as a loading control (A,E). (**B**) Semi-quantitative RT-PCR analyses of *HA-Maml1* using total RNA extracts prepared from each transfectant (labeled upper lane). G3PDH was used as the internal standard. (**C**,**D**) Whole-mount in situ hybridization analysis of E10.5 embryonic tails with DIG-labeled *Maml1* antisense (C) or sense (D) probes. Arrowheads indicate a newly formed boundary. (**E**) Schematic representation of the Flag-tagged Mesp2 mutants used for mapping of the region(s) involved in the inhibition of HA-Maml1 expression. The basic (blue), HLH (green) and degradation (red) domains of the Mesp2 protein are indicated. Right marks (○) or (×) in the scheme represent the occurrence of HA-Maml1 repression by each Flag-Mesp2 mutant. HA-Maml1 and the indicated Flag-Mesp2 mutants were introduced into NIH3T3 cells and detected by western blotting.

expression was also repressed by this mutant (Fig. 5E, lane 4). To further map the domain required for Maml1 suppression, we generated a series of truncated Mesp2 constructs and tested their ability to destabilize Maml1. Mesp2 proteins lacking the N-terminal domain (Mesp2AA83-370 and AA75-370) did not repress Maml1 expression (Fig. 5E, lanes 7 and 8), whereas AA70-370 retained the capacity to destabilize Maml1 (Fig. 5E, lane 9). Conversely, the N-terminal protein AA1-69 of Mesp2 was sufficient to destabilize Maml1, but a truncated product corresponding to amino acids AA1-60 lacked this repression activity (Fig. 5E, lanes 10 and 11), indicating that there are at least two crucial domains, AA61-69 and AA70-74, in Mesp2 (Fig. 5E). These findings thus strongly suggest that Mesp1 and Mesp2 promote the destabilization of Maml1 independently of their activity as transcription factors.

Maml1 colocalizes with Mesp2 in the nucleus and is repressed in situ

Another possible mechanism by which the destabilization of Maml1 occurred was translational suppression. To test this, we directly monitored Maml1 localization and stability ex vivo. After a 1-hour transfection with HA-Maml1 alone or Maml1 and either Flag-Mesp2 or a Flag-Mesp2 mutant (AA83-370), we monitored the time-course of cell population changes using antibodies against either HA or Flag. In the case of transfectants with HA-Maml1 only, Maml1 expression was detected as a very weak signal at 1 hour after a medium change (data not shown). The signal level and ratio increased thereafter and reached a saturated level after 4 hours. Maml1 expression was found to be stable because the rate of Maml1-expressing cells was unchanged from 4 to 16 hours (Fig. S5 in the supplementary material). In the case of co-transfection with Maml1 and Mesp2, three types of cells, expressing either Maml1 or Mesp2 or coexpressing both proteins, were observed. Interestingly, we found that Mesp2 completely colocalized with Maml1 as nuclear dots that probably correspond to PML bodies as it had been shown that Maml1 localizes in PML bodies (Fig. 6A) (Wu et al., 2000).

It was noted also that cells showing a lower signal for HA-Maml1 than for Flag-Mesp2 were observed only in the transfectants expressing wild-type Mesp2 (Fig. 6B) but not those harboring mutant-type Mesp2 (Fig. 6C). This indicated that HA-Maml1 is initially translated but might be repressed by Flag-Mesp2. In support of this possibility, the cell expression profile changed quickly and the number of cells showing coexpression of HA-Maml1 and Flag-Mesp2 decreased with time and cells expressing only Flag-Mesp2 become predominant after 16 hours (Fig. 6D, left). By contrast, in the Mesp2 mutant transfectants, the profile was almost unchanged with time (Fig. 6D, right) and HA-Maml1-positive cells (counted as HA single-positive and Flag and HA double-positive) were observed at a higher frequency compared with those in wild-type Mesp2 transfectants (Fig. 6). These observations led us to conclude that Mesp2 colocalizes with Maml1 in PML bodies and might facilitate their destabilization.

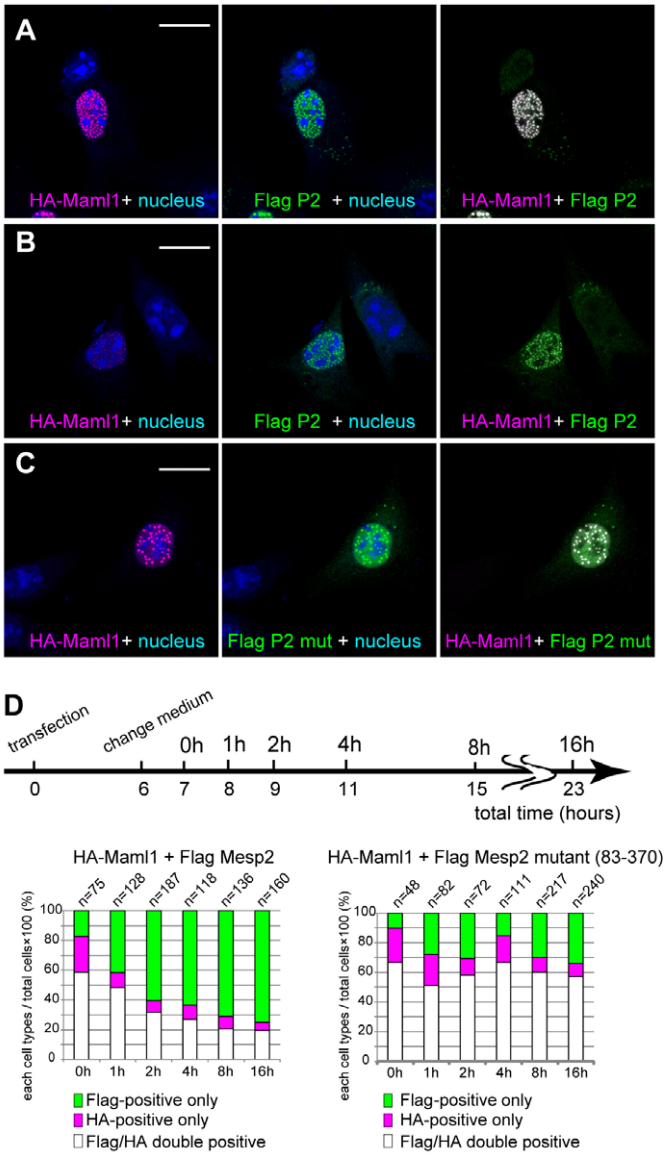

Fig. 6. Suppression of Maml1 expression ex vivo.
(**A-C**) Immunocytochemical analysis of HA-Maml1 with Flag-Mesp2 (A,B) or with a Flag-Mesp2 mutant (AA83-370; C) in NIH3T3 cells upon co-transfection. Images were taken at 11 hours after transfection (at the 4-hour harvesting time-point; see table in D). Maml1 (anti-HA, magenta), Mesp2 (anti-Flag, green) and nucleic acids (TOTO-3, blue) were detected. (**D**) Temporal changes in the cell population showing different expression patterns in NIH3T3 cells transfected with HA-Maml1 + Flag-Mesp2 (left) or a HA-Maml1 + Flag-Mesp2 mutant (AA83-370; right). Cells were collected at 0, 1, 2, 4, 8 or 16 hours after recovery from the transfection procedure (see timetable). The bar graphs indicate the ratio of cells expressing only Flag-Mesp2 or the Flag-Mesp2 mutant (green), HA-Maml1 (magenta), and HA-Maml1 and either Flag-Mesp2 or the Flag-Mesp2 mutant (white). The percentages shown are the average of two independent assays. The total cell numbers counted for each assay are indicated in the upper lanes. Scale bars: 20 μm.

Maml1 protein expression is repressed by Mesp2 during development

We finally evaluated whether Maml1 is also downregulated by Mesp2 in vivo and if this event makes any contribution to the mechanism underlying somite patterning, such as the establishment of RC polarity. Maml1 protein is also detectable as punctate nuclear signals in the mouse anterior PSM using anti-Maml1 antibodies (Fig. 7B,B′,D,D′,F,F′, magenta). If Maml1 is repressed by Mesp2 in vivo, the expression pattern of Maml1 would be expected to depend on the expression pattern of Mesp2, which is regulated by the cyclic changes in Notch signaling. We exhaustively examined the dynamic changes of the Maml1 protein expression that are related to changes in the Mesp2 protein expression profile in different Notch clock cycles in the wild-type PSM (Fig. 7A-F′). We used phases I, II and III as the Notch standard time according to the definition by Oginuma et al., which is assessed by the localization of NICD (Oginuma et al., 2008). As expected from our ex vivo analysis, Maml1 expression was significantly lower only in the Mesp2-expressing cells when compared with cells in other regions where Mesp2 is absent in all phases (Fig. 7A-F′). It was further noted that Maml1 protein was not yet affected in the domain with newly activated Mesp2 (Fig. 7F,F′, arrowheads). The repressive effects of Mesp2 were also supported by the analysis of *Mesp2*-null embryos in which Maml1 was expressed ubiquitously throughout the PSM (Fig. 7G).

Finally, we addressed whether Mesp2 generally acts as a repressor for the Notch signaling pathway via the repression of Maml1. To induce Mesp2 at the desired time-point in the entire body, we crossed a mouse line bearing heterozygous CAG-CAT-*Mesp2* with homozygous Cre-ERT2 mice that express a tamoxifen-inducible Cre-recombinase from the *Rosa26* locus (Fig. 7H) (Nakajima et al., 2006). We examined the Maml1 expression profile of each embryo recovered at E10.5 (one or two days after the administration of tamoxifen; Fig. 7I). In Cre-ERT2::CAG-CAT-*Mesp2* embryos treated with tamoxifen both at E8.5 and E9.5, the expression of *Mesp2* was ubiquitously upregulated in nearly all cells (Fig. 7 K,L). Whole embryo extracts were then used for western blot analyses. We found a clear reduction of Maml1 protein from Mesp2-misexpressing embryos (Cre-ERT2::CAG-CAT-*Mesp2*) compared with control embryos (Cre-ERT2::+; Fig. 7M). The double-transgenic embryos also showed malformed heart morphology and vascular network defects in the yolk sac, which are similar to phenotypes observed upon the loss of Notch signaling (Fig. 7K,L compared with 7J; data not shown). These observations strongly suggest that Mesp2 negatively regulates the Notch signaling pathway via the downregulation of Maml1 expression and that the rostral identity of a somite is established by this regulation within a rostral somite compartment (see model in Fig. 8A).

DISCUSSION

The negative regulation of Notch signaling is required at the anterior PSM where Mesp2 is expressed

From the results of our current study, we concluded that the activation of Notch signaling is precisely controlled by a distinct event downstream of Mesp2 during somitogenesis. We have previously shown that *Mesp2* is induced in the anterior PSM via Notch signaling and Tbx6 function (Yasuhiko et al., 2006). However, once Mesp2 is induced, the canonical Notch signaling pathway must be suppressed in the anterior compartment of a somite to establish the RC polarity. We have previously reported that *Lfng* induced by Mesp2 partly contributes to the suppression of Notch activity in the rostral compartment (Morimoto et al., 2005). However, defects in the *Mesp2*-null mice were not rescued by Lfng in a previous study (Oginuma et al., 2010), which is in contrast to the findings of our current experiments with R218H. Furthermore, we have shown that the RC patterning is generated without an NICD on/off state as long

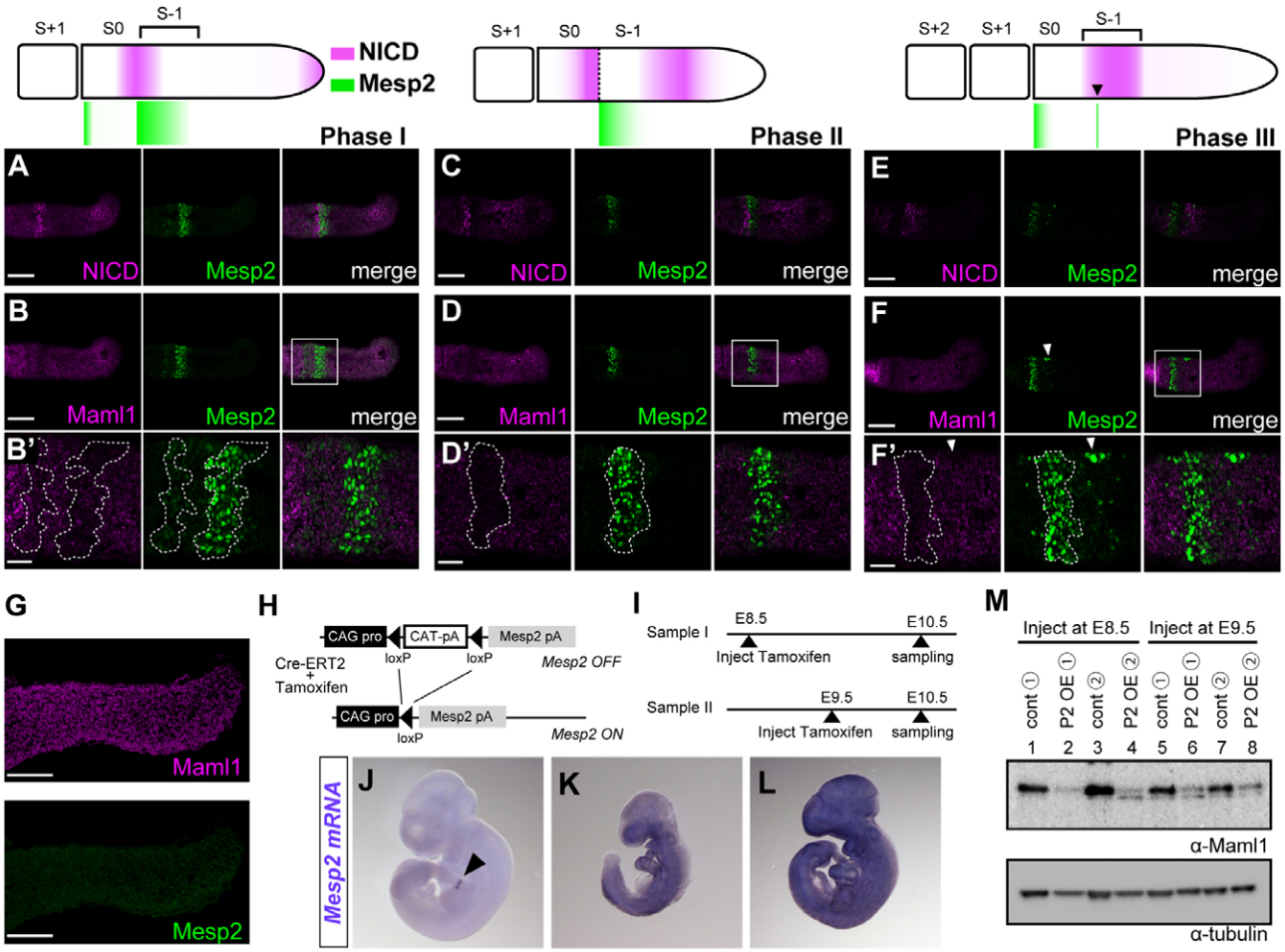

Fig. 7. Maml1 expression is downregulated by Mesp2 during normal somitogenesis and abnormal embryogenesis. (**A-F'**) Frozen serial sections (7 μm) of embryonic tail samples were used for double immunohistochemical analyses using anti-NICD (magenta) and anti-Mesp2 (green) antibodies (A,C,E) or anti-Maml1 (magenta) and anti-Mesp2 (green) antibodies (B,B′,D,D′,F,F′) during one cycle of somitogenesis (phase I, *n*=4/12; phase II, *n*=6/12; phase III, *n*=2/12). The area surrounded by white dots indicates the Mesp2-expressing region in which the expression level of Maml1 is weaker (B′,D′,F′). Arrowheads in the scheme for phase III (F,F′) show initial expression of Mesp2 proteins, and Maml1 expression is not downregulated in this region. The magnified images shown in the lower panels (B′,D′,F′) correspond to the boxed areas in B, D and F, respectively. (**G**) Double immunostaining images using antibodies against Maml1 (magenta) and Mesp2 (green) in *Mesp2*-null embryos (*n*=3). Maml1 is expressed in the entire PSM in *Mesp2*-null embryos. (**H**) Scheme for Tamoxifen-dependent recombination by Cre-ERT2, resulting in the ubiquitous misexpression of Mesp2 under the control of the CAG promoter. (**I**) The experimental schedule. (**J-L**) Whole-mount in situ hybridization using a *Mesp2* antisense probe. (J) Mesp2 is detected in the anterior PSM only in the control embryo (Cre-ERT2::+, arrowhead, *n*=12). (K,L) *Mesp2* is expressed grossly in *Mesp2*-misexpressing embryos (Cre-ERT2::CAG-CAT-*Mesp2*) treated with 3 mg Tamoxifen at E8.5 (K, *n*=2) or E9.5 (L, *n*=2). (**M**) Western blots of whole embryonic extracts. Mouse embryos expressing Cre-ER alone (shown as 'cont') or the combination of Cre-ER and *Mesp2* (shown as 'P2 OE') were assayed using two independent samples. Upper is Maml1, lower is tubulin. Scale bars: 100 μm in A-G; 40 μm in B′,D′,F′.

as Mesp2 is expressed at the presumptive rostral compartment (Oginuma et al., 2010). This indicates that the Mesp2 function downstream of NICD formation is crucial. We thus propose from our present data that Mesp2 might act as the final shut off switch for Notch signaling by disrupting the NICD-Maml1-Rbpj complex (Fig. 8A,B). As Maml1 is an essential component of the canonical Notch signaling pathway, its rapid turnover might be an effective way to locally suppress this signaling.

Mesp2 might affect other signaling pathways or transcriptional factor(s) via its suppression of Maml1 expression

Based on our present findings, we identified Maml1 as a target molecule of Mesp2. Previous studies in *Drosophila*, mice and human have demonstrated that Maml protein is an essential component of the NICD-Rbpj complex in the nucleus and might regulate Notch signaling at the transcriptional level (Helms et al., 1999; Kitagawa et al., 2001; Oyama et al., 2007; Shen et al., 2006; Smoller et al., 1990; Wu et al., 2000). Maml protein is also required for chromatin-dependent transactivation by the recombinant NICD-Rbpj enhancer complex in vitro and recruits CBP and p300 to promote nucleosome acetylation at Notch enhancers (Fryer et al., 2002). Furthermore, we speculate that Mesp2 acts as a negative regulator for other signaling pathways such as Wnt or p53 signaling as Maml1 is reported to act as a coactivator for β-catenin or p53 at their target sites (Alves-Guerra et al., 2007; Zhao et al., 2007). It is noteworthy in this regard that Wnt signaling has been reported to be involved in somite segmentation (Aulehla et al., 2008; Takada et al., 1994). We also have previously shown that the mRNA expression of *Lef1* (a nuclear effector of the Wnt/β-catenin

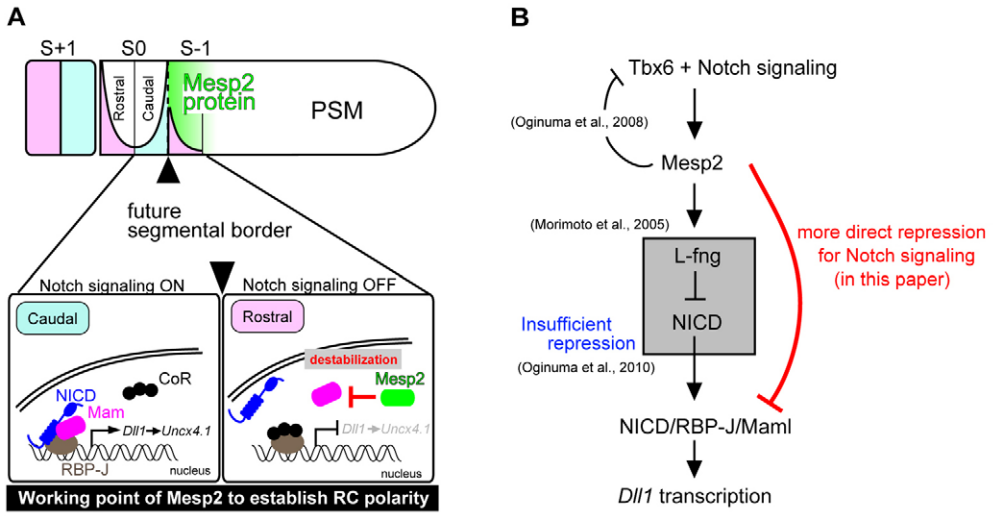

Fig. 8. A model for the establishment of rostro-caudal polarity within a somite. (**A**) Mesp2 protein (green) is expressed in the rostral half of the somite at S-1 under the control of Notch signaling. Once Mesp2 is expressed, however, it quickly suppresses Notch activity via the destabilization of Maml1, which leads to the failure of the ternary complex formation of NICD-Maml1-Rbpj (blue, magenta and gray, respectively). As a result, the transcription of downstream target genes of canonical Notch signaling is repressed by Rbpj with a co-repressor (black) in the rostral region. Conversely, Notch signaling target genes are upregulated in the caudal half region where Mesp2 expression falls below the threshold level. (**B**) Depiction of the genetic cascade involved in the regulation of Notch signaling during somitogenesis incorporating present and previous data. Mesp2 has three independent functions leading to (1) the induction of *Lfng* that represses the production of cleaved Notch1 (Morimoto et al., 2005), (2) the suppression of Tbx6 protein expression post-translationally (Oginuma et al., 2008), and (3) the repression of Maml1 protein via its destabilization (our present data). Although we have already reported that the repression of Notch signaling occurred via Lfng, which is induced by Mesp2, this suppression mechanism is insufficient to establish rostro-caudal polarity within a somite (Oginuma et al., 2010). We thus propose a novel mechanism by which Mesp2 represses Notch signaling, i.e. Mesp2 induces the destabilization of Maml1 protein independently of its function as a transcription factor.

signaling pathway) and *Axin2* (a target gene of Wnt/β-catenin signaling) are expanded at the anterior PSM in the *Mesp2*-null embryos (Ishikawa et al., 2004). Hence, it would be of interest in the future to investigate the possibility that Mesp2 might affect not only Notch signaling, but also the Wnt signaling pathway through the regulation of Maml1.

A novel molecular mechanism by which Mesp2 represses Maml1 expression

We also demonstrate from our present data that Mesp2 represses Maml1 protein independently of its function as a transcription factor. We investigated the step at which Maml1 is suppressed, i.e. the transcriptional, translational or post-translational level. The expression level of *Maml1* mRNA is unaffected by Mesp2, and Maml1 is also suppressed by the bHLH-domain-deletion mutant form of Mesp2 that cannot bind DNA directly (Fig. 5B-E), indicating that the repression does not occur at the transcriptional level. Translational suppression was also deemed to be improbable as Mesp2 localizes exclusively in the nucleus. To fully test this possibility, however, we attempted to monitor protein expression using antibodies against specific tags. Completely merged signals for Mesp2 and Maml1 were observed in the PML body, indicating that Maml1 protein could be translated even in the presence of Mesp2 protein. Consequently, we contend that Mesp2 represses Maml1 protein expression at the post-translational level.

It has already been reported that factors involved in mice somitogenesis are degraded by post-translational modification. Hes7, Mesp2 and Tbx6 were found to be quickly destabilized through ubiquitin-dependent proteolysis (Bessho et al., 2003; Morimoto et al., 2006; Oginuma et al., 2008). We therefore speculated that a post-translational process such as ubiquitination regulates Maml1. However, the destabilization of Maml1 by Mesp2 was not rescued by the addition of MG132 (see Fig. S4 in the supplementary material). Rather, the Maml1 protein levels were reduced when the cells were treated with MG132, even in the absence of Mesp2. We subsequently changed the treatment period and the concentration of MG132 but did not see any recovery over prolonged MG132 exposure; instead, this promoted the destabilization of Maml1. We thus now conclude that the proteasome pathway does not mediate the destabilization of Maml1 by Mesp2. An alternative destabilizing pathway might be lysosomal proteolysis but this pathway is primarily involved in endocytotic events, which are unlikely to play a role in the Mesp2 pathways as Mesp2 localizes only in the nucleus. In this regard, it should be noted that Mesp2 was found to colocalize with Maml1 in PML bodies and the suppression of Maml1 occurs as a result. As we also know that Mesp2 does not directly interact with Maml1 (data not shown), the identification of the mediating factor is a high priority in order to properly elucidate the mechanism underlying the temporal destabilization of Maml1.

Acknowledgements

We thank Tasuku Honjo and Hideyuki Okano for generously providing cDNA constructs. We are also grateful to Yuki Takahashi and Aya Satoh for their general assistance in maintaining the mouse colonies. This work is supported by Grants-in-Aid for Science Research on Priority Areas and the National BioResource Project of the Ministry of Education, Culture, Sports, Science and Technology, Japan. N.S. is supported by a postdoctoral fellowship from the National Institute of Genetics, Mishima, Japan.

Competing interests statement

The authors declare no competing financial interests.

Supplementary material

Supplementary material for this article is available at
http://dev.biologists.org/lookup/suppl/doi:10.1242/dev.055533/-/DC1

References

Alves-Guerra, M. C., Ronchini, C. and Capobianco, A. J. (2007). Mastermind-like 1 Is a specific coactivator of beta-catenin transcription activation and is essential for colon carcinoma cell survival. *Cancer Res.* **67**, 8690-8698.

Aoyama, H. and Asamoto, K. (1988). Determination of somite cells: independence of cell differentiation and morphogenesis. *Development* **104**, 15-28.

Aulehla, A., Wiegraebe, W., Baubet, V., Wahl, M. B., Deng, C., Taketo, M., Lewandoski, M. and Pourquie, O. (2008). A beta-catenin gradient links the clock and wavefront systems in mouse embryo segmentation. *Nat. Cell Biol.* **10**, 186-193.

Barrantes, I. B., Elia, A. J., Wunsch, K., Hrabe de Angelis, M. H., Mak, T. W., Rossant, J., Conlon, R. A., Gossler, A. and de la Pompa, J. L. (1999). Interaction between Notch signalling and Lunatic fringe during somite boundary formation in the mouse. *Curr. Biol.* **9**, 470-480.

Bessho, Y., Sakata, R., Komatsu, S., Shiota, K., Yamada, S. and Kageyama, R. (2001). Dynamic expression and essential functions of Hes7 in somite segmentation. *Genes Dev.* **15**, 2642-2647.

Bessho, Y., Hirata, H., Masamizu, Y. and Kageyama, R. (2003). Periodic repression by the bHLH factor Hes7 is an essential mechanism for the somite segmentation clock. *Genes Dev.* **17**, 1451-1456.

Bettenhausen, B., Hrabe de Angelis, M., Simon, D., Guenet, J. L. and Gossler, A. (1995). Transient and restricted expression during mouse embryogenesis of Dll1, a murine gene closely related to Drosophila Delta. *Development* **121**, 2407-2418.

Bussen, M., Petry, M., Schuster-Gossler, K., Leitges, M., Gossler, A. and Kispert, A. (2004). The T-box transcription factor Tbx18 maintains the separation of anterior and posterior somite compartments. *Genes Dev.* **18**, 1209-1221.

Chung, C. N., Hamaguchi, Y., Honjo, T. and Kawaichi, M. (1994). Site-directed mutagenesis study on DNA binding regions of the mouse homologue of Suppressor of Hairless, Rbpj kappa. *Nucleic Acids Res.* **22**, 2938-2944.

Dequeant, M. L. and Pourquie, O. (2008). Segmental patterning of the vertebrate embryonic axis. *Nat. Rev. Genet.* **9**, 370-382.

Evrard, Y. A., Lun, Y., Aulehla, A., Gan, L. and Johnson, R. L. (1998). lunatic fringe is an essential mediator of somite segmentation and patterning. *Nature* **394**, 377-381.

Feller, J., Schneider, A., Schuster-Gossler, K. and Gossler, A. (2008). Noncyclic Notch activity in the presomitic mesoderm demonstrates uncoupling of somite compartmentalization and boundary formation. *Genes Dev.* **22**, 2166-2171.

Fryer, C. J., Lamar, E., Turbachova, I., Kintner, C. and Jones, K. A. (2002). Mastermind mediates chromatin-specific transcription and turnover of the Notch enhancer complex. *Genes Dev.* **16**, 1397-1411.

Helms, W., Lee, H., Ammerman, M., Parks, A. L., Muskavitch, M. A. and Yedvobnick, B. (1999). Engineered truncations in the Drosophila mastermind protein disrupt Notch pathway function. *Dev. Biol.* **215**, 358-374.

Hicks, C., Johnston, S. H., diSibio, G., Collazo, A., Vogt, T. F. and Weinmaster, G. (2000). Fringe differentially modulates Jagged1 and Delta1 signalling through Notch1 and Notch2. *Nat. Cell Biol.* **2**, 515-520.

Ishikawa, A., Kitajima, S., Takahashi, Y., Kokubo, H., Kanno, J., Inoue, T. and Saga, Y. (2004). Mouse Nkd1, a Wnt antagonist, exhibits oscillatory gene expression in the PSM under the control of Notch signaling. *Mech. Dev.* **121**, 1443-1453.

Kato, H., Taniguchi, Y., Kurooka, H., Minoguchi, S., Sakai, T., Nomura-Okazaki, S., Tamura, K. and Honjo, T. (1997). Involvement of Rbpj in biological functions of mouse Notch1 and its derivatives. *Development* **124**, 4133-4141.

Kitagawa, M., Oyama, T., Kawashima, T., Yedvobnick, B., Kumar, A., Matsuno, K. and Harigaya, K. (2001). A human protein with sequence similarity to Drosophila mastermind coordinates the nuclear form of notch and a CSL protein to build a transcriptional activator complex on target promoters. *Mol. Cell. Biol.* **21**, 4337-4346.

Kohyama, J., Tokunaga, A., Fujita, Y., Miyoshi, H., Nagai, T., Miyawaki, A., Nakao, K., Matsuzaki, Y. and Okano, H. (2005). Visualization of spatiotemporal activation of Notch signaling: live monitoring and significance in neural development. *Dev. Biol.* **286**, 311-325.

Kraus, F., Haenig, B. and Kispert, A. (2001). Cloning and expression analysis of the mouse T-box gene tbx20. *Mech. Dev.* **100**, 87-91.

Lewis, J. (2008). From signals to patterns: space, time, and mathematics in developmental biology. *Science* **322**, 399-403.

Morimoto, M., Takahashi, Y., Endo, M. and Saga, Y. (2005). The Mesp2 transcription factor establishes segmental borders by suppressing Notch activity. *Nature* **435**, 354-359.

Morimoto, M., Kiso, M., Sasaki, N. and Saga, Y. (2006). Cooperative Mesp activity is required for normal somitogenesis along the anterior-posterior axis. *Dev. Biol.* **300**, 687-698.

Morimoto, M., Sasaki, N., Oginuma, M., Kiso, M., Igarashi, K., Aizaki, K., Kanno, J. and Saga, Y. (2007). The negative regulation of Mesp2 by mouse Ripply2 is required to establish the rostro-caudal patterning within a somite. *Development* **134**, 1561-1569.

Nakajima, Y., Morimoto, M., Takahashi, Y., Koseki, H. and Saga, Y. (2006). Identification of Epha4 enhancer required for segmental expression and the regulation by Mesp2. *Development* **133**, 2517-2525.

Oginuma, M., Niwa, Y., Chapman, D. L. and Saga, Y. (2008). Mesp2 and Tbx6 cooperatively create periodic patterns coupled with the clock machinery during mouse somitogenesis. *Development* **135**, 2555-2562.

Oginuma, M., Takahashi, Y., Kitajima, S., Kiso, M., Kanno, J., Kimura, A. and Saga, Y. (2010). The oscillation of Notch activation, but not its boundary, is required for somite border formation and rostral-caudal patterning within a somite. *Development* **137**, 1515-1522.

Oyama, T., Harigaya, K., Muradil, A., Hozumi, K., Habu, S., Oguro, H., Iwama, A., Matsuno, K., Sakamoto, R., Sato, M. et al. (2007). Mastermind-1 is required for Notch signal-dependent steps in lymphocyte development in vivo. *Proc. Natl. Acad. Sci. USA* **104**, 9764-9769.

Saga, Y. (1998). Genetic rescue of segmentation defect in MesP2-deficient mice by MesP1 gene replacement. *Mech. Dev.* **75**, 53-66.

Saga, Y. and Takeda, H. (2001). The making of the somite: molecular events in vertebrate segmentation. *Nat. Rev. Genet.* **2**, 835-845.

Saga, Y., Hata, N., Koseki, H. and Taketo, M. M. (1997). Mesp2: a novel mouse gene expressed in the presegmented mesoderm and essential for segmentation initiation. *Genes Dev* **11**, 1827-1839.

Shen, H., McElhinny, A. S., Cao, Y., Gao, P., Liu, J., Bronson, R., Griffin, J. D. and Wu, L. (2006). The Notch coactivator, MAML1, functions as a novel coactivator for MEF2C-mediated transcription and is required for normal myogenesis. *Genes Dev.* **20**, 675-688.

Smoller, D., Friedel, C., Schmid, A., Bettler, D., Lam, L. and Yedvobnick, B. (1990). The Drosophila neurogenic locus mastermind encodes a nuclear protein unusually rich in amino acid homopolymers. *Genes Dev.* **4**, 1688-1700.

Takada, S., Stark, K. L., Shea, M. J., Vassileva, G., McMahon, J. A. and McMahon, A. P. (1994). Wnt-3a regulates somite and tailbud formation in the mouse embryo. *Genes Dev.* **8**, 174-189.

Takahashi, J., Ohbayashi, A., Oginuma, M., Saito, D., Mochizuki, A., Saga, Y. and Takada, S. (2010). Analysis of Ripply1/2-deficient mouse embryos reveals a mechanism underlying the rostro-caudal patterning within a somite. *Dev. Biol.* **342**, 134-145.

Takahashi, Y., Koizumi, K., Takagi, A., Kitajima, S., Inoue, T., Koseki, H. and Saga, Y. (2000). Mesp2 initiates somite segmentation through the Notch signalling pathway. *Nat. Genet.* **25**, 390-396.

Takahashi, Y., Inoue, T., Gossler, A. and Saga, Y. (2003). Feedback loops comprising Dll1, Dll3 and Mesp2, and differential involvement of Psen1 are essential for rostrocaudal patterning of somites. *Development* **130**, 4259-4268.

Takahashi, Y., Hiraoka, S., Kitajima, S., Inoue, T., Kanno, J. and Saga, Y. (2005). Differential contributions of Mesp1 and Mesp2 to the epithelialization and rostro-caudal patterning of somites. *Development* **132**, 787-796.

Takahashi, Y., Yasuhiko, Y., Kitajima, S., Kanno, J. and Saga, Y. (2007). Appropriate suppression of Notch signaling by Mesp factors is essential for stripe pattern formation leading to segment boundary formation. *Dev. Biol.* **304**, 593-603.

White, P. H. and Chapman, D. L. (2005). Dll1 is a downstream target of Tbx6 in the paraxial mesoderm. *Genesis* **42**, 193-202.

Wu, L., Aster, J. C., Blacklow, S. C., Lake, R., Artavanis-Tsakonas, S. and Griffin, J. D. (2000). MAML1, a human homologue of Drosophila mastermind, is a transcriptional co-activator for NOTCH receptors. *Nat. Genet.* **26**, 484-489.

Yasuhiko, Y., Haraguchi, S., Kitajima, S., Takahashi, Y., Kanno, J. and Saga, Y. (2006). Tbx6-mediated Notch signaling controls somite-specific Mesp2 expression. *Proc. Natl. Acad. Sci. USA* **103**, 3651-3656.

Zhang, N. and Gridley, T. (1998). Defects in somite formation in lunatic fringe-deficient mice. *Nature* **394**, 374-377.

Zhao, Y., Katzman, R. B., Delmolino, L. M., Bhat, I., Zhang, Y., Gurumurthy, C. B., Germaniuk-Kurowska, A., Reddi, H. V., Solomon, A., Zeng, M. S. et al. (2007). The notch regulator MAML1 interacts with p53 and functions as a coactivator. *J. Biol. Chem.* **282**, 11969-11981.